Selin, Markus; Nummelin, Sami; Deleu, Jill; Ropponen, Jarmo; Viitala, Tapani; Lahtinen, Manu; Koivisto, Jari; Hirvonen, Jouni; Peltonen, Leena; Kostiainen, Mauri A.; Bimbo, Luis M.

High-Generation Amphiphilic Janus-Dendrimers as Stabilizing Agents for Drug Suspensions

Published in:
Biomacromolecules

DOI:
10.1021/acs.biomac.8b00931

Published: 28/08/2018

Document Version
Publisher's PDF, also known as Version of record

Article

Cite This: Biomacromolecules 2018, 19, 3983−3993

pubs.acs.org/Biomac

High-Generation Amphiphilic Janus-Dendrimers as Stabilizing Agents for Drug Suspensions

Markus Selin,[*,†] Sami Nummelin,[*,‡] Jill Deleu,[†,§] Jarmo Ropponen,[∥] Tapani Viitala,[⊥] Manu Lahtinen,[#] Jari Koivisto,[▽] Jouni Hirvonen,[†] Leena Peltonen,[†] Mauri A. Kostiainen,[‡,○] and Luis M. Bimbo[*,†,◆]

[†]Division of Pharmaceutical Chemistry and Technology, Faculty of Pharmacy, University of Helsinki, FI-00014, Finland
[‡]Biohybrid Materials, Department of Bioproducts and Biosystems, Aalto University, FI-00076, Finland
[§]Faculty of Pharmaceutical Sciences, Ghent University, 9000 Ghent, Belgium
[∥]VTT-Technical Research Centre of Finland Ltd, P.O. Box 1000, FI-02044 VTT Finland
[⊥]Division of Pharmaceutical Biosciences, Faculty of Pharmacy, University of Helsinki, FI-00014, Finland
[#]Department of Chemistry, University of Jyväskylä, FI-40014, Finland
[▽]Department of Chemistry and Materials Science, Aalto University, FI-00076, Finland
[○]HYBER Center of Excellence, Department of Applied Physics, Aalto University, FI-00076, Finland
[◆]Strathclyde Institute of Pharmacy and Biomedical Sciences, University of Strathclyde, Glasgow, G4 ORE, United Kingdom

Supporting Information

ABSTRACT: Pharmaceutical nanosuspensions are formed when drug crystals are suspended in aqueous media in the presence of stabilizers. This technology offers a convenient way to enhance the dissolution of poorly water-soluble drug compounds. The stabilizers exert their action through electrostatic or steric interactions, however, the molecular requirements of stabilizing agents have not been studied extensively. Here, four structurally related amphiphilic Janus-dendrimers were synthesized and screened to determine the roles of different macromolecular domains on the stabilization of drug crystals. Physical interaction and nanomilling experiments have substantiated that Janus-dendrimers with fourth generation hydrophilic dendrons were superior to third generation analogues and Poloxamer 188 in stabilizing indomethacin suspensions. Contact angle and surface plasmon resonance measurements support the hypothesis that Janus-dendrimers bind to indomethacin surfaces via hydrophobic interactions and that the number of hydrophobic alkyl tails determines the adsorption kinetics of the Janus-dendrimers. The results showed that amphiphilic Janus-dendrimers adsorb onto drug particles and thus can be used to provide steric stabilization against aggregation and recrystallization. The modular synthetic route for new amphiphilic Janus-dendrimers offers, thus, for the first time a versatile platform for stable general-use stabilizing agents of drug suspensions.

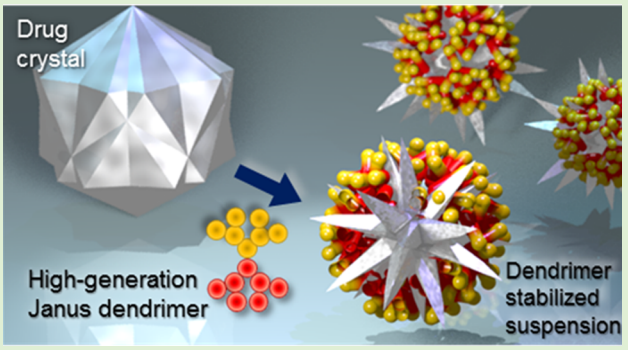

1. INTRODUCTION

Many newly developed active pharmaceutical ingredients (APIs) are poorly soluble in water as well as in biological fluids. Drug nanocrystals in which the particle size of a drug is nanosized to increase its surface area were developed to circumvent this solubility issue.[1] Media milling is currently a widely used method to reduce particle size, which in turn increases the APIs' surface area and the surface-specific drug dissolution rate. However, drug nanocrystals tend to form aggregates or to coalesce due to the Ostwald ripening phenomenon.[2,3] It is postulated that if a dense enough steric stabilizer layer is formed around drug particles dispersed in solution, the formation of van der Waals forces is hindered and the drug particles remain separated from each other. Hence, drug crystals must be stabilized using a polymer or a surfactant coating that increases repulsive electrostatic interactions, steric strain, and shelf life during storage. The advantage of stabilized drug nanocrystals is that the majority of the formulated product consists of drug material, which is not easily achievable with other types of carrier-systems.[4] Moreover, the use of stabilized nanocrystals improves drug bioavailability by other means, for example, via enhanced mucoadhesion and efflux

Received: June 14, 2018
Revised: August 27, 2018
Published: August 28, 2018

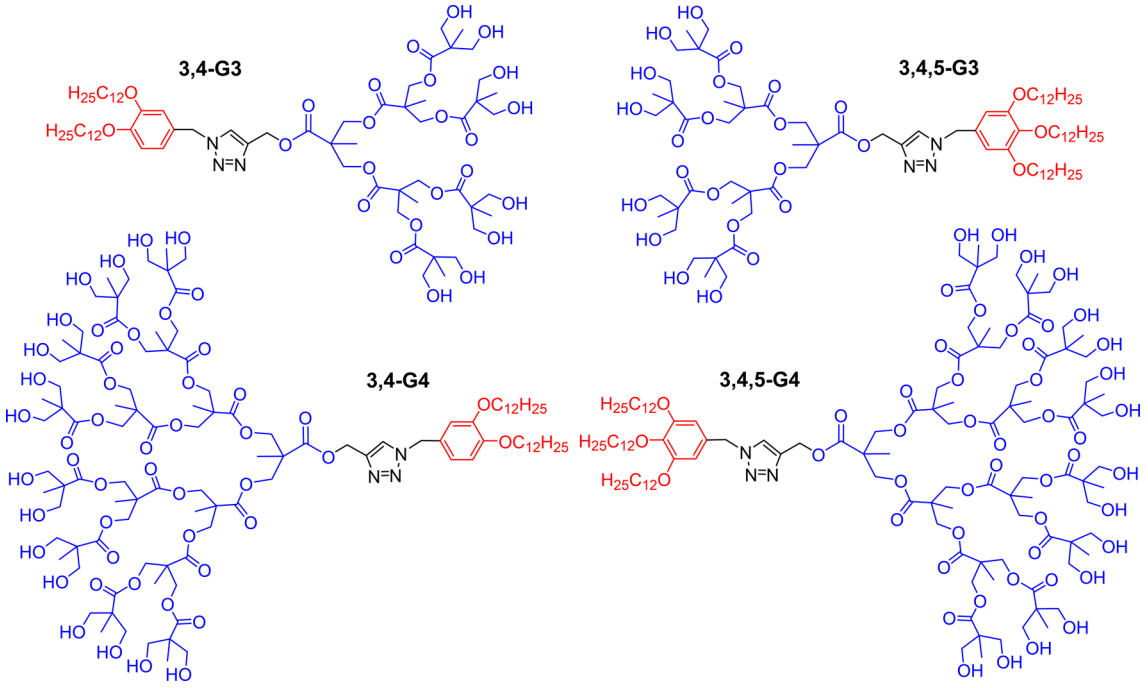

Figure 1. Chemical structures and short notation of the Janus-dendrimers evaluated in this study.

inhibition.[5] Screening methods for the production and subsequent analyses of nanosuspensions are limited,[6] and few pharmaceutically accepted excipients are currently utilized as stabilizers.[7] Amphiphilic copolymers in which the different domains of the polymer have affinity toward either the adsorbent (particle surface) or dispersion medium have been found to be suitable steric stabilizers. Among the various copolymers used for drug particle stabilization, Poloxamer 188, a nonionic triblock copolymer composed of a hydrophobic polyoxypropylene chain edged by two hydrophilic polyoxyethylene chains, is one of the most widely used and studied.

Dendrimers are a class of well-defined, periodically branched macromolecules[8−10] in which a recurrent branching of the building blocks originating from a core results in a core−shell structure.[11,12] Intrinsic structural features of dendrimers allow for the covalent conjugation of drug molecules or complexations through multivalent noncovalent interactions.[13−15] Amphiphilic Janus-dendrimers (JDs)[16−19] are essentially synthetic surfactants, which combine hydrophilic and hydrophobic dendritic domains into a single macromolecule. Their structural versatility is demonstrated by the different families of JDs[17,20−24] and Janus-glycodendrimers.[25−28] When injected from dilute organic solutions into aqueous or biological media, some JDs readily self-assemble into bilayered, vesicle-like structures, that is, dendrimersomes[17,29] and glycodendrimersomes,[30−33] or other complex architectures.[17,34,35] The shape and size of these assemblies can be controlled and even predicted using existing semiempirical models.[36−38] Several dendrimer compositions[39] have been employed in diverse biomedical applications,[40] for example, as a coating for 3D DNA nanostructures for improved stability against endonucleases,[41] as antibacterial agents with minimal eukaryotic cell toxicity,[42] as sealants for wound closure,[43] and as supramolecular hydrogels for sustained drug release.[44]

Here we hypothesized that high-generation amphiphilic JDs, which have a high density of hydroxyl-terminated bis-MPA dendrons per molecule while at the same time exhibit hydrophobic dodecyloxy chains, could be prime candidates for stabilizing colloidal drug suspensions through steric stabilization. The aim of the study was to investigate if high-generation JDs could be effectively used to stabilize drug suspensions of the poorly water-soluble drugs indomethacin and itraconozale and compare their performance with Poloxamer 188. The study describes for the first time the mechanisms by which amphiphilic JDs stabilize pharmaceutical drug suspensions and the influence of the number of hydrophobic alkyl tails in the adsorption kinetics of the JDs to drug crystals in suspension.

2. EXPERIMENTAL SECTION

Materials. All reagents and solvents used in the synthesis of JDs were obtained from commercial sources (Acros, Aldrich, Fisher, and Rathburn; reagent grade) and were used without prior purification. Dry dichloromethane (CH_2Cl_2) and tetrahydrofuran (THF), which were used for the synthesis of intermediate compounds, were obtained from a solvent drier (MB-SPS-800, neutral alumina; MBraun, Germany) and used when necessary. The deuterated DMSO-d_6 for NMR analysis was purchased from Euriso-top (Saint Aubin Cedex, France). Propargyl-modified bis-MPA dendrons (G1−G4) were synthesized according to Wu et al. (**3, 5, 7, 9** Supplementary Scheme S1).[45] Percec-type hydrophobic G1 azide dendrons were prepared according to Nummelin et al. (**14a, b** Supplementary Scheme S2).[44,46] Amphiphilic JDs 3,4-G3 and 3,4,5-G3 (Figure 1) were prepared as described previously.[44] The characterization data were in agreement with the literature. Itraconazole (Derivados Quimicos Fine Chemicals, Spain) and indomethacin (Orion Pharma, Finland) were used as model drugs. Poloxamer 188 (BASF, Germany) was used as a model stabilizer (positive control). Potassium hydroxide and acetic acid (Sigma-Aldrich, Germany) were used to make the acetic acid buffer at pH 5.00. Ethanol (99.5%; Altia, Finland) was used as a solvent for indomethacin during the ultraviolet (UV) spectroscopy measurements. Magnesium stearate (Orion Pharma, Finland) was used as a lubricant during the tableting procedure for the contact angle measurements. Ultrapure water (18.2 MΩ·cm) was obtained from Millipore Elix 5 equipment (Merck, France).

DOI: 10.1021/acs.biomac.8b00931
Biomacromolecules 2018, 19, 3983−3993

Synthesis and Characterization of Janus-Dendrimers. *General Procedure.* The azide dendron **14a** or **14b** (1.05 equiv), G3 or G4 bis-MPA-alkyne **7** or **9** (1 equiv), and sodium L-ascorbate (20 mol %) were dissolved in THF in a vial. Cu(II)SO_4 (10 mol %) was dissolved in H_2O and added to the reaction. The mixture was stirred for 5 min at RT before DMSO was added. The mixture was stirred 24 h at 60 °C before it was cooled to RT. The crude product was purified by flash chromatography on SiO_2, affording Janus-dendrimers as off-white solids (see Supporting Information Schemes S1−S4 for details).

Nuclear Magnetic Resonance (NMR). ^{1}H NMR (400 MHz) spectra and uniform driven equilibrium Fourier transform (UDEFT, pulse program: *udeft*) ^{13}C NMR (100 MHz) spectra were recorded on a Bruker Avance DPX400 spectrometer equipped with a 5 mm BBFO probehead. Chemical shifts (δ) were reported in ppm (Figures S1−S4). The residual protic solvent of DMSO-d_6 (^{1}H, δ 2.50 ppm; ^{13}C, δ 39.50 ppm) was used as the internal reference. Coupling constants (J) were reported in Hertz (Hz). Heteronuclear ^{1}H-^{13}C connectivities were determined by adiabatic HSQC experiments (pulse program: *hsqcetgpsisp.2*).

Matrix-Assisted Laser Desorption/Ionization Time-of-Flight Mass Spectrometry (MALDI-TOF). The analyses were carried out using a Bruker UltrafleXtreme MALDI-TOF/TOF mass spectrometer (Bruker Daltoniks, Bremen, Germany) equipped with a SmartBeam II laser (355 nm) operating at 2 kHz with a 200 μm raster in reflectron positive mode. FlexAnalysis v3.4 was used to assign molecular isotopic masses in the 200−4000 Da mass range. 2,5-Dihydroxybenzoic acid (DHB) mixed in a THF (10 mg mL^{-1}) was used as a matrix. A concentration of 2 mg mL^{-1} of the sample in THF was mixed with the matrix solutions in 1:1 (v/v) ratio and applied to the stainless steel target plate. Sample droplets were dried under a gentle air stream at room temperature to obtain small crystals that simplified ionizaton. A peptide calibration standard II (Bruker starter kit # 8208241) was used for calibration.

Thermal Analysis. For each JD, a physical mixture with bulk indomethacin was prepared by weighing and mixing 20.0 mg of the bulk drug and 2.0 mg of a solid dendrimer, respectively. The resulting mixtures, as well as neat JDs and indomethacin, were then subjected to thermal analysis. Thermal transitions were measured using a Mettler Toledo 823e (Switzerland) differential scanning calorimeter and were processed using STARe software (Mettler Toledo, version 9.00). Samples (3−7 mg) were annealed for 5 min at 25 °C before they were heated to 190 °C at 10 °C min^{-1} heating rate. Nitrogen was used as a purge gas at a 50 mL min^{-1} flow rate. Thermal transitions as peak maximas (°C) and enthalpies (kcal mol^{-1}) are reported in Supporting Information Tables S2 and S3. Indium was used as a calibration standard both for temperature and enthalpy. Melting points for the 3,4-G4 and 3,4,5-G4 JDs were taken as the maxima of the endothermic peaks.

Contact Angle. Aqueous dendrimer solutions (0.4 mg mL^{-1}), an aqueous poloxamer solution (1.0 mg mL^{-1}), and water were used for the contact angle measurements. The contact angles were measured on cylindrical drug compacts produced from 300 mg bulk indomethacin in an infrared spectroscopy pellet (⌀ 13 mm) by applying one ton compression for 10 s using an Atlas 15.001 manual hydraulic press (SPECAC, England). A sample solution droplet (about 2 μL) was deposited onto an indomethacin compact, and images were captured once per second for 1 min using a Cam200 Contact Angle Meter (KSV Instruments, Finland) and were processed using Attension Theta software (Biolin Scientific, version 4.1.0). The average and standard deviation of the contact angles are presented as functions of time.

Surface Plasmon Resonance. The interactions of indomethacin with 3,4-G4, 3,4,5-G4, and the poloxamer reference were determined by surface plasmon resonance (SPR) measurements performed using a 4-channel multiparametric MP-SPR 200 instrument (BioNavis, Finland) equipped with a 670 nm laser and a peristaltic pump (Ismatec, Germany). Indomethacin was deposited onto gold SPR sensor surfaces from aliquots of a saturated indomethacin solution that was preprepared by shaking indomethacin in ethanol (4 mg mL^{-1}) overnight. The SPR signal baseline was first recorded in pure water, and the SPR sensograms were obtained by recording the change in the SPR angle approximately every 5.3 s during 50 μM aqueous stabilizer solution injection for 15 min (association phase) and subsequently during pure water injection for at least an additional 15 min (dissociation phase). For comparison, the SPR measurements were repeated with plain gold sensors alone. The recorded data were baseline corrected using the background data and were modeled using Matlab R2014a software (MathWorks, version 8.3.0.532) with an in-house algorithm that removes measurement disturbances with a simple input method and optimizes the range of time points to fit the exponential decay models to the association and dissociation phases.

Manual Milling. Bulk indomethacin or itraconazole (4.0 mg) were placed in a glass test tube with 3.0 g of zirconium oxide beads (⌀ 1 mm), and 1 mL of the aqueous stabilizer solution was used as the milling medium. The tube was capped, and the bulk drug was manually milled utilizing vortex-mixing: 60 s continuous milling periods and 15 s pauses were alternated until the total milling time reached 6 min. Longer manual milling times were not required for the screening, as it has been shown that the rate of particle size reduction decreases during extended milling periods.[6]

Particle Preparation. The indomethacin suspensions were manually milled in aqueous dendrimer solutions (0.40 mg mL^{-1}) and were stored at RT. An aqueous poloxamer solution (1.00 mg mL^{-1}) was used as the milling medium for the positive controls and water without excipients was used as the milling medium for the negative controls. In order to separate any JD aggregates from the drug particles, all four JD solutions were also subjected to a manual milling process without indomethacin and were monitored in parallel with the indomethacin suspensions.

Particle Sizing. Particle size was measured using dynamic light scattering (DLS). The milled drug suspensions were vortex-mixed for 30 s, diluted 40-fold with water, and briefly mixed again prior to subjecting the dilutions to the DLS analysis in a disposable plastic cuvette. Z-average size and PDI were recorded. DLS analyses were performed at 25 °C using a Zetasizer Nano ZS (Malvern Instruments, U.K.) equipped with 4 mW He−Ne laser 633 nm and an avalanche photodiode positioned at 173° to the beam. Instrument parameters and measurement times were determined automatically. The size was determined based on an average of 12 measurement runs in triplicate.

Stability Studies. After milling, the suspensions were subjected to particle size analysis for 4 weeks. During the first week, the repeatability of the milling process was followed with three separately milled samples. From the second to the fourth week, the particle size of a single sample was monitored weekly.

Redispersion Studies. For the redispersion studies, two separately milled suspensions were pooled, and 700 μL of the suspension was dried on well plates in an oven for 4 d at 40 °C. Saturated aqueous indomethacin solutions were subsequently prepared and filtered. The dried samples were dispersed in 700 μL aliquots of the saturated indomethacin solutions, followed by 3 min of sonication (35 kHz) prior to subjecting the redispersed suspensions to particle size analysis.

UV Spectrophotometry. The UV absorption spectra of 40 μg mL^{-1} indomethacin in ethanol and 100 μg mL^{-1} 3,4-G4 in water (Figure S5) were recorded from 190 to 400 nm using a quartz cuvette and a UV-1600PC spectrophotometer (VWR international, China) to select wavelengths for subsequent UV determinations. At 318.5 nm, indomethacin has a local absorbance maximum and the absorbance of the dendrimer is at minimum. Therefore, this wavelength was selected for the determination of indomethacin content in solutions with the dendrimers. Accordingly, the indomethacin content in the milled suspensions was determined as follows: 10 μL of each suspension was dissolved in 990 μL of ethanol, and then the indomethacin content of the solutions was determined using a calibration curve (318.5 nm wavelength). The drug content in each suspension was calculated based on triplicate measurements.

At 260.3 nm, indomethacin has high absorbance values and the dendrimer has a local absorption minimum, whereas at 280.0 nm the absorbance of indomethacin is reduced and the dendrimer has a local

DOI: 10.1021/acs.biomac.8b00931
Biomacromolecules 2018, 19, 3983−3993

absorption maximum. Monitoring absorbance at 260.3 nm allows for the estimation of indomethacin content that is below the lower limit of detection at 318.5 nm. In such a case, the influence of the dendrimer concentration on the results should be monitored based on the absorbance values at 280.0 nm. Finally, neither indomethacin nor the dendrimer absorb light at a 400 nm wavelength. In theory, light scattering due to particulate matter in the samples can distort the UV determinations. Thus, the absorbance of each sample was also measured at a 400.0 nm wavelength.

Saturation Solubility. Bulk indomethacin (10.0 mg) was weighed into glass vessels, and 1.5 mL of a 12 mM acetate buffer (pH 5.0) was added to the vessels. Next, 0.5 mL of aqueous dendrimer solution (0.4 mg mL^{-1}), aqueous poloxamer solution (1.0 mg mL^{-1}), or water was added. The vessel was sealed tightly, placed for overhead shaking in a REAX 2 shaker (Heidolph, Germany) for 24 h at RT, and allowed to stand for 12 h before the solution was filtered through a 0.2 μm filter. The absorbance of the filtered solution was determined at four predefined wavelengths. The indomethacin content was determined using a UV spectroscopy calibration curve (260.3 nm). The concentration of indomethacin in the saturated solution, as well as the absorbance at 280.0 nm were recorded.

Dissolution Rate. Dissolution experiments were conducted with 500 mL of a 12 mM acetate buffer (pH 5.0) stirred (50 rpm) using a DT6 dissolution apparatus (Erweka, Germany) in an ET 15001 (Erweka, Germany) heat bath at 37 °C. Independently milled indomethacin suspensions were stored at RT for 1 d before subjecting them to the dissolution experiment. Each measurement with the suspensions began with placing 500 μL of a vortex-mixed suspension into the dissolution chamber of the apparatus. The dissolution experiments with bulk indomethacin began with measuring 2.0 mg of nonmilled indomethacin powder into the dissolution vessel and pouring 500 mL of a prewarmed, 12 mM acetate buffer (pH 5.0) into the vessel at the start of the experiment. The dissolution process was monitored as a function of time by taking 1 mL aliquots from the dissolution media at defined time points. The indomethacin content in the samples was determined using a UV spectroscopy calibration curve (318.5 nm). The extent of dissolution was calculated for the dissolution samples at each time point, and the averages and standard deviations of the dissolution profiles were calculated and reported.

3. RESULTS AND DISCUSSION

Screening Study Design. To validate the manual milling methodology for the screening studies, indomethacin was media-milled in an aqueous Poloxamer 188 solution (positive control) and in water (negative control). For the manual milling method, the initial Z-average size was 1231 nm for the positive control and 814 nm for the negative control. The positive control was selected on the basis of earlier studies: when indomethacin is mechanically milled using poloxamer as the stabilizer, monodisperse submicron drug particles are obtained.[47] The presence of poloxamer in the samples should not influence the DLS results by changing the viscosity of the dispersant, as a 2000-fold concentration increase only changes the viscosity of the aqueous solution to 1.26 mPas[48] from about 0.89 mPas (the viscosity of plain water at RT). Therefore, the difference in the initial sizes of the controls should reflect a successful adsorption of poloxamer onto the indomethacin particles or a slightly reduced milling efficiency. After 3 weeks of storage at RT, the Z-average size of the positive control only showed a moderate increase (+121 nm) compared to the negative control (+3667 nm). Small-scale manual milling reduced the size of the particles in indomethacin suspensions, and the suspensions were successfully stabilized by the poloxamer (positive control). Hence, it was concluded that this experimental approach could be used in screening studies involving JDs.

A preliminary screening of JDs with two different drugs (indomethacin and itraconazole) was conducted to confirm their particle size-stabilizing efficiency and the proper concentration of dendrimer solutions, as well as to select the model drug for further investigations. Three different concentrations of 3,4-G4 were used in the screenings, as follows: low (0.04 mg mL^{-1}), medium (0.10 mg mL^{-1}), and high (0.40 mg mL^{-1}). Additionally, poloxamer was also investigated as a stabilizer for both indomethacin and itraconazole at a concentration of 1.0 mg mL^{-1} to provide a benchmark for the JDs. Manually milled indomethacin and itraconazole suspensions were stored at 4 °C for 138 and 144 days, respectively. After four months of storage, all the suspensions were subjected to particle size analysis, and as a conclusion indomethacin suspensions showed smaller Z-average size and narrower size distribution than itraconazole suspensions and poloxamer-stabilized suspensions (Figure S6). The observed low reproducibility of this screening method, especially in the case of itraconazole, is assumed to be due to the manual milling procedure and the hardness of the drug compound. Mechanization of the process, together with longer milling times, is expected to decrease the variability of the results. The conservation of the smaller Z-average for extended periods of time is one of the hallmarks of successful drug particle stabilization.[5] Poloxamer was found to prevent agglomeration during the four month storage and under our experimental conditions the JDs performed equally or better with only a fraction of the concentration required for poloxamer. This is thought to be due to the high density of hydroxyl-terminated bis-MPA dendrons per molecule which leads to a strong physical barrier on the particles' surface that hinders the attractive van der Waals' forces between particles. Furthermore, the mechanical milling procedure of bulk indomethacin required less time and material in contrast to bulk itraconazole, which required at least two grams of material.[49] Therefore, indomethacin was selected as the sole model drug to be further studied with the four different types of JDs, namely G3 and G4 both with 3,4- and 3,4,5-branching (Table S1). The data collected from the preliminary screenings led us to choose a 1:10 dendrimer-to-drug mass-ratio for preparing the forthcoming indomethacin suspensions by manual milling.

Interaction Studies. The thermal behavior of the pristine JDs and the JD-indomethacin physical mixtures (JD/IND = 1:10) were analyzed using differential scanning calorimetry (DSC) to discern physical interactions and the chemical compatibility of the mixtures. All dendrimers, except 3,4-G3, displayed a broad melting transition (>6 kcal mol^{-1}) preceded by one or two weaker endothermic transitions (Figure 2, Table S2), which most likely indicate a small-scale structural rearrangement (solid-state phase transition) of the dendritic branches. The 3,4,5-branched JDs generally showed about 20 °C higher melting points than their 3,4-branched analogues. In the case of 3,4-G3, due to its amorphous nature a glass transition (ΔC_p = 0.08 kcal mol^{-1} K^{-1}) was observed at 94.3 °C accompanied by a structural relaxation (enthalpic) peak on top of it. Moreover, 3,4,5-G3, and 3,4,5-G4 dendrimers exhibited liquid crystal phases, as weak endothermic isotropization transitions were observed in the DSC curves at 169.8 and 152.8 °C, respectively. Neat indomethacin showed only a sharp melting transition (T_m) at 160.4 °C (T_e = 159.3 °C), which corresponds with the melting temperature of the crystalline γ-form of indomethacin.[50]

DOI: 10.1021/acs.biomac.8b00931
Biomacromolecules 2018, 19, 3983−3993

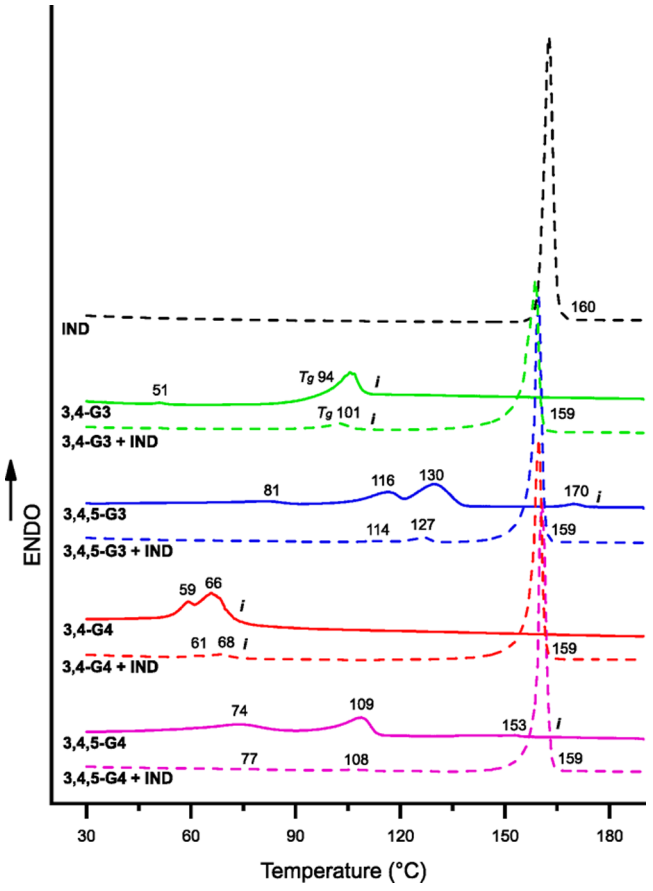

Figure 2. DSC curves [10 °C min^{-1}] of Janus dendrimers (colored solid line), indomethacin (black dashed line), and physical mixtures of Janus dendrimers (10 wt %) and indomethacin (colored dashed line). Transition temperatures are marked in each curve as peak maxima [°C].

Physical mixtures of the JDs and indomethacin systematically exhibited the same endothermic transitions corresponding with those previously observed for their individual components, as evidenced by the DSC curves (Figure 2 and Table S3). Generally, the endotherms of the dendrimer components become somewhat more difficult to observe in the scans as the weight fraction of the JDs, and consequently, the magnitude of transitions, became only 1:10 that of pristine JDs. Nonetheless, only the isotropization peak of the LC phase of 3,4,5-G4 (152.8 °C) was missing in the DSC curve but was likely buried underneath the broadened indomethacin melting peak and thus not evident. Predictably, the melting transitions of indomethacin showed somewhat broader melting ranges and small downward shifts in peak maxima (1.0−1.5 °C). This phenomenon is caused by the well-known "impurity effect", which occurs when small amounts of a foreign substance are added to a pure component, and it is commonly reported for physical mixtures of stabilized drugs as well. For example, the shift from 165.0 to 133.6 °C (50:50) and 112.3 °C (30:70) has been reported for indomethacin and poloxamer mixtures.[51] In conclusion, the absence of major discrepancies in the thermal events confirms that JDs and indomethacin do not show eutectic melting behavior, cocrystal formation, or induction of polymorphs because indomethacin remains in crystalline γ-form. In addition, the overall crystallinity of the JD-indomethacin mixtures remained unchanged after mixing.

As discussed by Bakatselou et al.,[52] surfactants may promote the wetting of drug particles, thereby increasing the drug dissolution rate. Therefore, contact angle measurements of aqueous solution droplets on compressed indomethacin surfaces were carried out to investigate the wettability of the drug when in contact with different JDs and the poloxamer (Figure 3). The procedure mimics the media milling

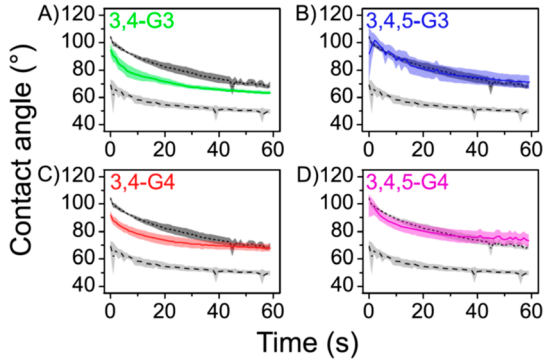

Figure 3. Contact angle of a drop of aqueous (A) 3,4-G3, (B) 3,4,5-G3, (C) 3,4-G4, and (D) 3,4,5-G4 solution (0.4 mg mL^{-1} deposited onto an indomethacin tablet; solid line ± colored area), aqueous poloxamer solution (1.0 mg mL^{-1}; line with long dashes ± light gray area), and water (line with short dashes ± dark gray area). Chemical structures are abbreviated with colored text. The solid line curves are the average of three separate measurements ± standard deviation, represented as the colored area.

conditions in which solid drug particles are dispersed in aqueous stabilizer solutions. The measured contact angles of water and the aqueous poloxamer solution were in agreement with the literature data.[47] The contact angles measured between the dendrimer solutions and indomethacin were consistently higher than the contact angles between poloxamer solution and indomethacin. In general, the contact angles between aqueous dendrimer solutions and indomethacin were comparable to the contact angle values between plain water and indomethacin at the end of the experiment. In contrast, the contact angle between the 3,4-G3 solution and indomethacin was slightly lower than the contact angle between water and indomethacin. A careful examination of the contact angles as a function of time revealed that the contact angles of samples that contained 3,4-G3 and 3,4-G4 JDs decreased faster than the contact angle values between water and indomethacin. The contact angles of 3,4,5-G3 and 3,4,5-G4 followed the contact angle values between water and indomethacin throughout all experiments. Studies investigating hydrocarbon materials have suggested that contact angles between liquids and coated solid materials reflect the properties of the solvent-exposed chemical groups of the coatings rather than those of the bulk solid.[53,54] Accordingly, if a drop of an aqueous solution of a stabilizer has a lower contact angle on the indomethacin surface than a drop of water, a decrease in the contact angle value due to the presence of dissolved stabilizers should reflect reductions in the solid−liquid and liquid−vapor interfacial energies caused by the adsorption of the materials onto these interfaces. As the dendrimers with fewer aliphatic chains in the hydrophobic dendron (3,4-G3 and 3,4-G4, as opposed to 3,4,5-G3 and 3,4,5-G4) displayed some surface-active characteristics under these experimental conditions, it is assumed that these

DOI: 10.1021/acs.biomac.8b00931
Biomacromolecules 2018, 19, 3983−3993

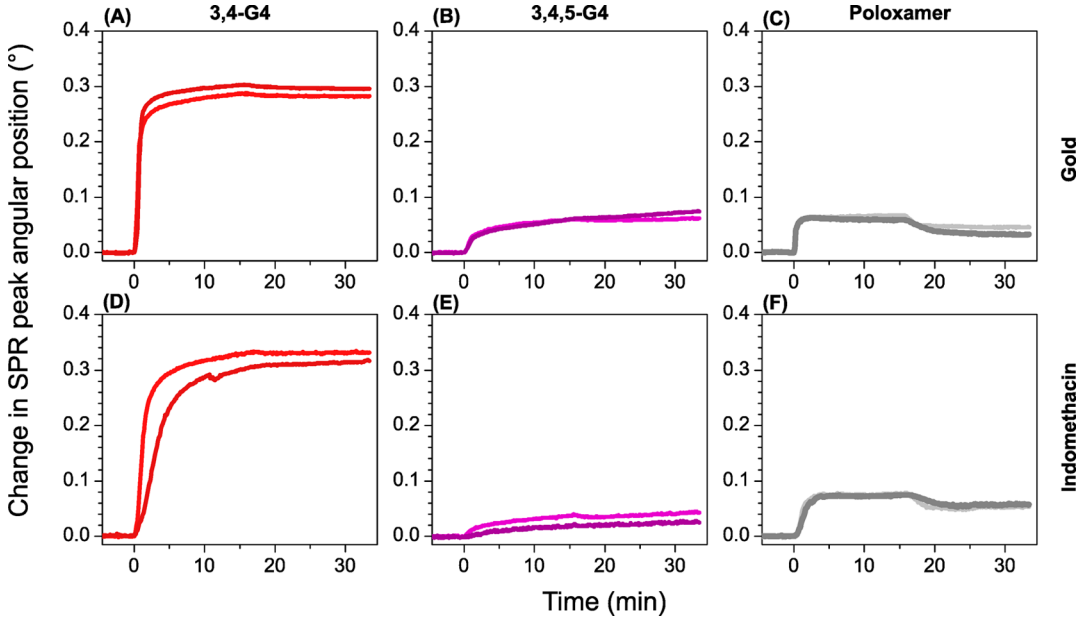

Figure 4. SPR angle data for 3,4-G4 (A,D), 3,4,5-G4 (B,E), and poloxamer (C,F) for measurements conducted on pure gold (A−C) and indomethacin covered (D−F) SPR sensors. The association phases (the first 15 min) preceded the dissociation phases (from 15 to 33.4 min). The two different curves in each panel are repeated measurements of the same system.

dendrimers enable drug particle wetting to a greater extent which could aid the dissolution process. However, none of the dendrimers achieved the same reduction in contact angle as the poloxamer.

The interactions between the drug and dendrimers were further studied using MP-SPR to identify the solid−liquid interface interactions independent of the interactions at the liquid−air and solid−air interfaces. In general, G4 JDs and poloxamer adsorbed onto plain gold (Figure 4A−C) and indomethacin surfaces (Figure 4D−F). The injection of G3 JDs did not result in detectable changes in the SPR peak angular positions (data not shown). The G4 JDs showed very little or no desorption from plain gold or indomethacin surfaces (Figure 4A,B and D,E), whereas poloxamer clearly desorbed from the surfaces (Figure 4C,F). Because the SPR peak angular position values were above the baseline levels at the end of the poloxamer desorption process, it was concluded that the desorbed fraction of the poloxamer molecules were incompletely attached to the surfaces or were only entangled with other poloxamer molecules. The dendrimers did not desorb from the surfaces, which indicates that a steady-state SPR peak angular position in the adsorption phase was reached due to surface saturation. For each sample, the adsorption onto the indomethacin surface was slower than onto the plain gold surface. Moreover, the poloxamer sample was the fastest and the 3,4,5-G4 sample the slowest to reach steady-state values during SPR responses (Figure S7). Changes in SPR responses arise when the molecules in the aqueous phase are adsorbed onto the sensor and cause refractive index changes near the surface. In detail, the binding events are converted to a change in the measurable sensor output value at efficiency, which depends on the recognition element and the analyzed compound. Therefore, the magnitude of the SPR responses should not be directly compared between chemically distinct samples; however, as the 3,4,5-G4 has a structure related to 3,4-G4 and also showed slower adsorption kinetics, it is postulated that the bulkier hydrophobic domain (3 alkyl tails vs. 2 alkyl tails) sterically hinders the packing of 3,4,5-G4 on the surfaces. The ideal features of a steric stabilizer in terms of steric hindrance rely on the affinity of the stabilizer to the particle surface as well as to the dispersant.[7] In addition, polymeric steric stabilization does not usually destroy the crystal structure of drug particles, unlike the action of conventional small molecular weight surfactants, for example, sodium dodecyl sulfate (SDS). The irreversible adsorption of the JDs to the indomethacin surfaces corroborates the hypothesis that the stabilization of drug particles occurs mainly due to steric hindrance and not by decrease of the surface tension in which little to no adsorption would take place.

Particle Size Stabilization. Next, the particle size reduction and the stabilization of the indomethacin suspensions were screened in the presence of dendrimers using DLS. Four and 7 days after milling, the Z-average size of the suspension milled in the presence of 3,4-G3 showed the largest Z-average size values (8549 ± 2853 and 9346 ± 2481 nm, respectively), which is a clear indication of aggregation. The Z-average sizes of the suspensions with 3,4,5-G3 (2228 ± 631 and 2334 ± 161 nm), 3,4-G4 (1084 ± 128 and 1561 ± 659 nm), and 3,4,5-G4 (1983 ± 475 and 1937 ± 352 nm) were noticeably smaller and mostly nonaggregated.

Indomethacin suspensions in aqueous dendrimer solutions (samples) and dendrimers solutions alone (background controls) were milled and monitored weekly over a four-week period (Figures 5 and S8) to examine the stability of the coated drug particles. In general, the samples showed larger Z-average sizes than the background controls. Considering this and the ratios of the sample components, the Z-average sizes of the samples should mainly reflect the Z-average size of the indomethacin crystals in the suspensions. A closer examination of the results from indomethacin milled in the presence of 3,4-G3 revealed that during the four-week period the measured Z-average sizes showed large variations (3049 nm) and considerably irregular developments (Figure 5A). In contrast, the Z-average size of the indomethacin suspensions milled with

DOI: 10.1021/acs.biomac.8b00931
Biomacromolecules 2018, 19, 3983−3993

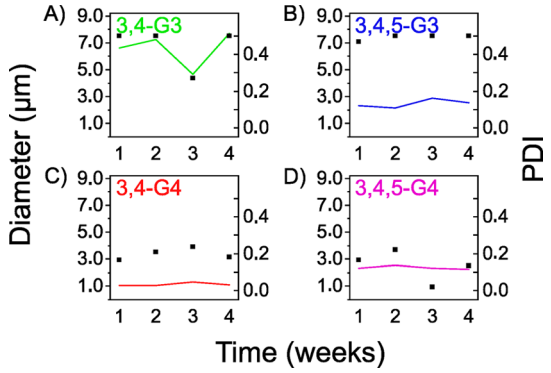

Figure 5. Development of the Z-average size (left axis, line) and PDI (right axis, squares) of an aqueous (A) 3,4-G3, (B) 3,4,5-G3, (C) 3,4-G4, and (D) 3,4,5-G4 solutions milled with indomethacin. Chemical structures abbreviated with colored text.

3,4,5-G3, 3,4-G4, and 3,4,5-G4 (Figure 5B–D) varied less over the four-week period, increasing 690, 283, and 259 nm, respectively. For 3,4,5-G3, the comparatively high uniformity and abundance of small JDs' background structures in the control measurements (Figure S8) raised a question regarding the potential bias in the stability results, which is discussed later in the text. Structure–activity comparisons between the dendrimers with the 3,4-hydrophobic dendron (3,4-G3 and 3,4-G4) suggested that the G4 hydrophilic dendron is required for particle stabilization. In conclusion, the 3,4-G3 showed the weakest performance as a stabilizer, whereas repeatable and stable indomethacin particles were obtained in the presence of G4 JDs. The results demonstrate the potential of G4 JDs to stabilize drugs in submicron suspensions at low dendrimer-to-drug mass ratios.

Suspensions obtained through media milling are often formulated as dry dosage forms. To obtain dosage forms with enhanced dissolution behaviors, the reduced size of the particles should be maintained through downstream processing, dry storage, and subsequent redispersion. To study the stabilizing performance of the dendrimers in this context, the milled indomethacin suspensions were dried, and the particle sizes were determined after redispersion (Figure 6). In the presence of the dendrimers and poloxamer, the indomethacin particles had a Z-average size ranging from about 1 to 4 μm after drying and redispersion. In the absence of these materials, indomethacin particles had a Z-average size of about 27 μm.

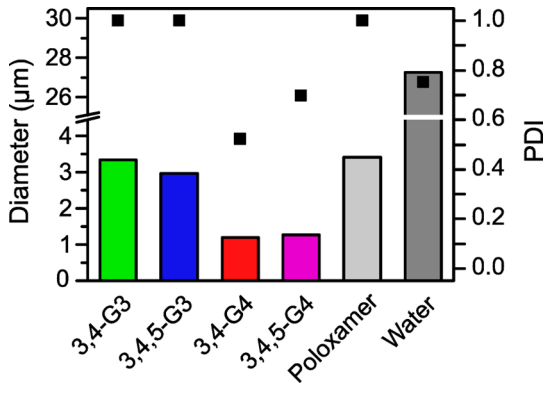

Figure 6. Z-average size (left axis, colored area) and PDI (right axis, black squares) after drying and redispersion of indomethacin suspensions milled in the presence sample materials (n = 1).

The best stabilizing performances were observed for G4 JDs. It should also be noted that the dry state stabilizing performances of the G3 JDs were as good as the stabilizing performance of the poloxamer.

Saturation Solubility. To examine the solubilizing potential of the dendrimers, solubilized indomethacin contents were determined from aqueous solutions saturated with an excess of the bulk drug (Table 1). The apparent solubility of indomethacin was moderately increased in buffer solutions supplemented with the dendrimers compared to the solubility in plain buffer. The absorbance values of 3,4-G4 containing saturation solubility samples at a 280 nm wavelength were about 2% of the values expected based on the UV spectrum recorded from the 3,4-G4 (Figure S5). This could indicate that a majority of the dendrimers was adsorbed onto nondissolved, bulk drug particles and then removed during filtration. Considering the absorbance values of the other samples at 280 nm, the same held true for the other dendrimers, including 3,4,5-G3 which formed background nanostructures in aqueous solutions. The formation of background structures was not considered when interpreting the results of the contact angle measurements. The formation of self-associated nanostructures might compete against 3,4,5-G3 adsorption on the surfaces of an aqueous drop thereby reducing the ability of the dendrimer to influence the contact angle. However, the lack of dissolved 3,4,5-G3 in the saturation solubility experiment supported the initial interpretations of the contact angle data, and contradicted the existence of the self-associated background structures in the milled indomethacin suspensions stabilized with 3,4,5-G3, thereby confirming the particle size stabilizing potential of the JDs.

Table 1. Solubility of Indomethacin and Absorbance at 280.0 nm Measured in 2 mL of 9 mM Acetate Buffer (pH 5.0) Supplemented with Indomethacin and the Solubilizing Agents (n = 1)[a]

solubilizing agent		UV spectroscopy results	
Janus-dendrimer or control	content [mg mL^{-1}]	indomethacin solubility [μg L^{-1}]	absorbance [AAU]
3,4-G3	0.30	590.1	0.0175
3,4,5-G3	0.30	434.3	0.0104
3,4-G4	0.30	493.5	0.0134
3,4,5-G4	0.30	557.2	0.0170
poloxamer	0.75	541.8	0.0121
none	N/A	401.4	0.0107

[a]Abbreviations: not applicable (N/A), arbitrary absorbance unit (AAU).

The solubility of indomethacin in a plain pH 5.0 buffer was 1 order of magnitude lower than a value reported in the literature[55] but well in line with indomethacin solubility in acidified water at RT,[56] however, water solubility over 1 order of magnitude higher (16 mg L^{-1}) has also been suggested for indomethacin.[48] The variations in the values reported in the literature might reflect the pH sensitivity of the solubility determinations close to the pK_a value of indomethacin (4.3),[57] the temperature dependence of indomethacin solubility,[58] the differences in the dissolution characteristics of indomethacin polymorphs,[59] and the effects of the experimental methodologies.[60]

Dissolution Rate. The dissolution of indomethacin reached 90% of the indomethacin contents within 3 min in

DOI: 10.1021/acs.biomac.8b00931
Biomacromolecules 2018, 19, 3983–3993

all samples milled in the presence of dendrimers and poloxamer (Figure 7A–D), and the extent of dissolution in

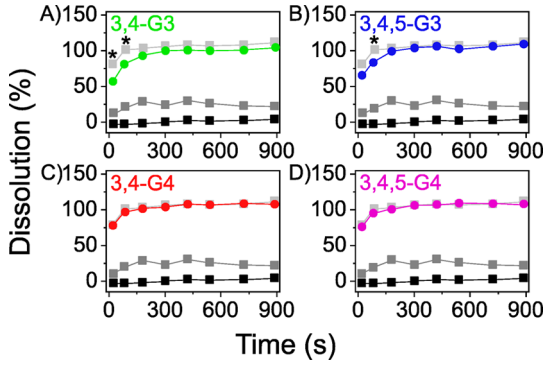

Figure 7. Dissolution results of (A) 3,4-G3, (B) 3,4,5-G3, (C) 3,4-G4, and (D) 3,4,5-G4 samples (colored circles), the poloxamer control (light gray squares), negative control (gray squares ± gray area) and bulk drug (black squares) as measured at 318.5 nm wavelength (n = 3). The asterisk represents significant differences between the sample and the poloxamer control (p = 0.05). Chemical structures abbreviated with colored text.

these samples did not decrease over the measured period. In contrast, the dissolution of indomethacin milled in water reached only 30% of the indomethacin content within 3 min and decreased to 22% at the end of the experiment. For further comparison, bulk indomethacin (nonmilled drug powder) reached 4% dissolution within the time frame of the experiment. The extent of bulk indomethacin dissolution agreed with the extent of dissolution expected at an equilibrium state (roughly 10%). Conversely, the maximum extent of dissolution observed for the negative control in the dissolution experiment (30%) greatly exceeded the measured saturation solubility.

The dissolution of indomethacin (Figure 7) co-occurred with the disappearance of drug particles scattering light (Figure S9). Scattering was not evident in the results of indomethacin milled without any stabilizer or bulk indomethacin. For the remainder of the milled indomethacin suspensions, the recorded absorbance values at 400 nm were small and sloped downward during the first 3 min of the experiment. This indicates that light scattering can be detected using this method and that scattering should only slightly affect the intensity of the light transmitted through the samples at the beginning of the experiment when a large number of particles is present and a majority of the drug has not yet dissolved. In general, the results indicate that milling enhances the dissolution of indomethacin and that the dendrimers can stabilize the indomethacin suspensions produced by milling.

The samples milled in the presence of 3,4-G3 and 3,4,5-G3 (Figure 7A,B) showed slightly slower dissolution rates compared to the poloxamer control, whereas the samples milled in the presence of 3,4-G4 and 3,4,5-G4 (Figure 7C,D) showed dissolution rates comparable to the poloxamer control. It is noteworthy that indomethacin particles stabilized with 3,4,5-G3 and 3,4,5-G4 had comparable Z-average sizes, but the particles stabilized with 3,4,5-G4 reached 90% dissolution faster than the particles stabilized with 3,4,5-G3. As both JDs have 3,4,5-substituted hydrophobic dendrons and there might be a bias in the 3,4,5-G3 size results, only a speculative structure–activity comparison of the hydrophilic dendrons is given at this stage. The 3,4,5-G3 has less hydrogen bond donors and acceptors than 3,4,5-G4, which might lead to slower kinetics in the coating desorption and a simultaneous decrease in the dissolution of indomethacin. The average extent of indomethacin dissolution in the samples containing 3,4-G3 did not reach as high percentage values as the samples containing the other dendrimers (Figure 7). Also, the particles persisted longer in the 3,4-G3-containing samples than in the poloxamer control and the samples stabilized with the other dendrimers (Figure S9). In order to maintain a steric barrier that is able to minimize interparticle interactions to a level that the attractive van der Waals forces are lower than the repulsive steric forces, the stabilizing moiety needs to be sufficiently long and dense.[3] The less dense hydroxyl-terminated bis-MPA dendron of the G3 JDs is therefore less efficient in promoting steric stabilization as the G4 JDs, which have double the hydroxyl-terminated bis-MPA groups. Therefore, a higher Z-average size and polydispersity is observed for G3-stabilized drug particles compared to the G4-stabilized ones (Figure 5), as well as a lower efficiency in promoting drug dissolution (Figure 7).

Solubility Enhancement. The reduction of particle size during the media milling process increases the total surface area of indomethacin and improves the rate of dissolution according to the Noyes–Whitney equation. Moreover, size reduction has also been shown to increase the surface specific dissolution rate.[61] The suggested mechanism relies on interpreting the combined effect of the particle size's dependent terms according to the Prandtl boundary layer equation for flat surfaces (eq S1), viz. dissolving boundary layer length (L) and the velocity of the solvent in relation to the dissolving surface (V), as the correlated reduction of the hydrodynamic boundary layer thickness (h_H) and the distance of molecular diffusion in the dissolution process. According to Keck and Müller,[62] saturation solubility increases as the equilibrium between dissolution and recrystallization shifts due to increasing dissolution rates. Therefore, the enhanced solubility of indomethacin in the negative control of the dissolution experiment is the result of size reduction (Figure 6). For the other samples in the dissolution experiment, the observed enhancement of solubility may be due to the combined effect of the size reduction and the presence of solubilizing and wetting agents.[52,58] As previously noted, the contact angles between aqueous dendrimer solutions and indomethacin surfaces were relatively high, which indicates that the dendrimers do not influence the wetting of indomethacin. Moreover, assuming a constant ratio between the amounts of the solubilizing agent and the increments in the solubilized indomethacin content (Table 1), the size reduction seems to largely dictate the extent of solubility enhancement.

Enhanced solubility is maintained in the stabilized indomethacin suspensions with broad particle size distributions, especially in samples containing 3,4-G3 (Figures 5A and 7A). This may be explained by applying a polymeric net crystal growth inhibition model, which relies on the Kelvin equation, to the dendrimer coated drug crystals in the suspensions.[63] In essence, even a partial coverage of the seed crystal surfaces is enough to inhibit crystal growth. According to the rationale presented, the size reduction also enhances the dissolution rate of the dendritic coatings on size-reduced particles with high surface curvatures. Hence, while the coatings and the drug molecules of the small particles dissolve rapidly, the coatings of the larger particles should persist longer and should slow the

DOI: 10.1021/acs.biomac.8b00931
Biomacromolecules 2018, 19, 3983–3993

recrystallization of indomethacin. An apparent lack of recrystallization might also be caused by the slow kinetics of indomethacin recrystallization,[64] however the slow indomethacin recrystallization in the stabilized samples reflects a shortage of noncoated seed crystal facets in the dissolution media, as the extent of dissolution sloped downward in the negative control but not in the stabilized suspensions during the dissolution experiment.

4. CONCLUSIONS

High-generation amphiphilic JDs (G3 and G4) obtained via a copper-catalyzed click-chemistry reaction using a modular synthesis approach were used to screen submicron drug crystal stabilization. The screening methodology applied minimizes the use of stabilizing materials, and the results demonstrate a good applicability of the G4 JDs as stabilizers in media milling and the subsequent dry-state processing of pharmaceuticals. The dense steric layer induced by the hydroxyl terminated bis-MPA dendrons in the G4 JDs plays a critical role in the stabilization process preventing the drug particles' agglomeration for extended periods of time, while enabling low polydispersity values when compared with G3 JDs and Poloxamer 188. Further, the SPR measurements support the hypothesis that JDs irreversibly adsorb onto the indomethacin surfaces via hydrophobic interactions and that the number of hydrophobic alkyl tails determine the adsorption kinetics of the JDs. In addition, both G4 JDs increase the drug dissolution rate of poorly water-soluble compounds to the same extent as the poloxamer at a lower stabilizer-to-drug ratio. We thus believe that the modular synthesis approach for JDs described here offers a convenient and efficient route for the stabilization of poorly water-soluble drugs in suspension. As a result, we envisage that these structures may be further tailored and scaled-up for pharmaceutical processing purposes.

■ ASSOCIATED CONTENT

Supporting Information

The Supporting Information is available free of charge on the ACS Publications website at DOI: 10.1021/acs.biomac.8b00931.

Synthesis details (Scheme S1–S4), ^{1}H NMR and ^{13}C NMR spectra (Figures S1 and S3), adiabatic HSQC 2D NMR spectra (Figures S2 and S4), UV spectra (Figure S5), sample usage (Table S1), preliminary screening results (Figure S6), thermal transitions and enthalpies (Table S2 and S3), average rate parameter values and magnitude of SPR peak angular position shift (Figure S7), development of Z-average size over time (Figure S8), and scattering-induced absorbance values in samples (Figure S9) (PDF)

■ AUTHOR INFORMATION

Corresponding Authors

*E-mail: markus.selin@helsinki.fi.
*E-mail: sami.nummelin@aalto.fi.
*E-mail: luis.bimbo@strath.ac.uk.

ORCID

Sami Nummelin: 0000-0003-2195-4818
Tapani Viitala: 0000-0001-9074-9450
Mauri A. Kostiainen: 0000-0002-8282-2379
Luis M. Bimbo: 0000-0002-8876-8297

Notes

The authors declare no competing financial interest.

■ ACKNOWLEDGMENTS

Financial support by the Academy of Finland (no. 276377 for L.M.B., no. 268616 for J.R., and nos. 263504, 267497, and 273645 for M.A.K.), the Sigrid Jusélius Foundation, the Magnus Ehrnrooth Foundation, the Emil Aaltonen Foundation, the Finnish Cultural Foundation, Orion Research Foundation, and Jane and Aatos Erkko Foundation is gratefully acknowledged. The work was carried out under the Academy of Finland's Centres of Excellence Programme (2014-2019).

■ REFERENCES

(1) Müller, R. H.; Keck, C. M. Twenty Years of Drug Nanocrystals: Where Are We, and Where Do We Go? *Eur. J. Pharm. Biopharm.* **2012**, *80* (1), 1–3.
(2) Rabinow, B. E. Nanosuspensions in Drug Delivery. *Nat. Rev. Drug Discovery* **2004**, *3* (9), 785–796.
(3) Wu, L.; Zhang, J.; Watanabe, W. Physical and Chemical Stability of Drug Nanoparticles. *Adv. Drug Delivery Rev.* **2011**, *63* (6), 456–469.
(4) Nguyen, T. T. C.; Nguyen, C. K.; Nguyen, T. H.; Tran, N. Q. Highly Lipophilic Pluronics-Conjugated Polyamidoamine Dendrimer Nanocarriers as Potential Delivery System for Hydrophobic Drugs. *Mater. Sci. Eng., C* **2017**, *70* (2), 992–999.
(5) Tuomela, A.; Hirvonen, J.; Peltonen, L. Stabilizing Agents for Drug Nanocrystals: Effect on Bioavailability. *Pharmaceutics* **2016**, *8* (2), 16.
(6) Van Eerdenbrugh, B.; Stuyven, B.; Froyen, L.; Van Humbeeck, J.; Martens, J. A.; Augustijns, P.; Van den Mooter, G. Downscaling Drug Nanosuspension Production: Processing Aspects and Physicochemical Characterization. *AAPS PharmSciTech* **2009**, *10* (1), 44–53.
(7) Peltonen, L.; Hirvonen, J. Pharmaceutical Nanocrystals by Nanomilling: Critical Process Parameters, Particle Fracturing and Stabilization Methods. *J. Pharm. Pharmacol.* **2010**, *62* (11), 1569–1579.
(8) Bosman, A. W.; Janssen, H. M.; Meijer, E. W. About Dendrimers: Structure, Physical Properties, and Applications. *Chem. Rev.* **1999**, *99* (7), 1665–1688.
(9) Caminade, A. M.; Laurent, R.; Majoral, J. P. Characterization of Dendrimers. *Adv. Drug Delivery Rev.* **2005**, *57* (15), 2130–2146.
(10) Tomalia, D. A.; Christensen, J. B.; Boas, U. *Dendrimers, Dendrons and Dendritic Polymers*; Tomalia, D. A., Christensen, J. B., Boas, U., Ed.; Cambridge University Press: New York, 2012.
(11) Sun, H.-J.; Zhang, S.; Percec, V. From Structure to Function via Complex Supramolecular Dendrimer Systems. *Chem. Soc. Rev.* **2015**, *44* (12), 3900–3923.
(12) Tomalia, D. A. Dendrons/Dendrimers: Quantized, Nano-Element like Building Blocks for Soft-Soft and Soft-Hard Nano-Compound Synthesis. *Soft Matter* **2010**, *6* (3), 456–474.
(13) Khandare, J.; Calderón, M.; Dagia, N. M.; Haag, R. Multifunctional Dendritic Polymers in Nanomedicine: Opportunities and Challenges. *Chem. Soc. Rev.* **2012**, *41* (7), 2824–2848.
(14) Menjoge, A. R.; Kannan, R. M.; Tomalia, D. A. Dendrimer-Based Drug and Imaging Conjugates: Design Considerations for Nanomedical Applications. *Drug Discovery Today* **2010**, *15* (5–6), 171–185.
(15) Lee, C. C.; MacKay, J. A.; Fréchet, J. M. J.; Szoka, F. C. Designing Dendrimers for Biological Applications. *Nat. Biotechnol.* **2005**, *23* (12), 1517–1526.
(16) Caminade, A.-M.; Laurent, R.; Delavaux-Nicot, B.; Majoral, J.-P. Janus" Dendrimers: Syntheses and Properties. *New J. Chem.* **2012**, *36* (2), 217–226.
(17) Percec, V.; Wilson, D. A.; Leowanawat, P.; Wilson, C. J.; Hughes, A. D.; Kaucher, M. S.; Hammer, D. A.; Levine, D. H.; Kim,

DOI: 10.1021/acs.biomac.8b00931
Biomacromolecules 2018, 19, 3983–3993

A. J.; Bates, F. S.; Davis, K. P.; Lodge, T. P.; Klein, M. L.; DeVane, R. H.; Aqad, E.; Rosen, B. M.; Argintaru, A. O.; Sienkowska, M. J.; Rissanen, K.; Nummelin, S.; Ropponen, J. Self-Assembly of Janus Dendrimers into Uniform Dendrimersomes and Other Complex Architectures. *Science* **2010**, *328* (5981), 1009−1014.
(18) Ropponen, J.; Nummelin, S.; Rissanen, K. Bisfunctionalized Janus Molecules. *Org. Lett.* **2004**, *6* (15), 2495−2497.
(19) Tomalia, D. A.; Pulgam, V. R.; Swanson, D. R.; Huang, B. Janus Dendrimers and Dendrons. U.S. Patent 7,977,452 B2, 2011.
(20) Nummelin, S.; Selin, M.; Legrand, S.; Ropponen, J.; Seitsonen, J.; Nykänen, A.; Koivisto, J.; Hirvonen, J.; Kostiainen, M. A.; Bimbo, L. M. Modular Synthesis of Self-Assembling Janus-Dendrimers and Facile Preparation of Drug-Loaded Dendrimersomes. *Nanoscale* **2017**, *9* (21), 7189−7198.
(21) Filippi, M.; Patrucco, D.; Martinelli, J.; Botta, M.; Castro-Hartmann, P.; Tei, L.; Terreno, E. Novel Stable Dendrimersome Formulation for Safe Bioimaging Applications. *Nanoscale* **2015**, *7* (30), 12943−12954.
(22) Liu, X.; Zhou, J.; Yu, T.; Chen, C.; Cheng, Q.; Sengupta, K.; Huang, Y.; Li, H.; Liu, C.; Wang, Y.; Posocco, P.; Wang, M.; Cui, Q.; Giorgio, S.; Fermeglia, M.; Qu, F.; Pricl, S.; Liang, Z.; Rocchi, P.; Rossi, J. J.; Peng, L. Adaptive Amphiphilic Dendrimer-Based Nanoassemblies as Robust and Versatile SiRNA Delivery Systems. *Angew. Chem., Int. Ed.* **2014**, *53* (44), 11822−11827.
(23) Nazemi, A.; Gillies, E. R. Dendrimersomes with Photodegradable Membranes for Triggered Release of Hydrophilic and Hydrophobic Cargo. *Chem. Commun.* **2014**, *50* (76), 11122−11125.
(24) Mikkilä, J.; Rosilo, H.; Nummelin, S.; Seitsonen, J.; Ruokolainen, J.; Kostiainen, M. A. Janus-Dendrimer-Mediated Formation of Crystalline Virus Assemblies. *ACS Macro Lett.* **2013**, *2* (8), 720−724.
(25) Xiao, Q.; Zhang, S.; Wang, Z.; Sherman, S. E.; Moussodia, R.-O.; Peterca, M.; Muncan, A.; Williams, D. R.; Hammer, D. A.; Vértesy, S.; Andre, S.; Gabius, H.-J.; Klein, M. L.; Percec, V. Onion-like Glycodendrimersomes from Sequence-Defined Janus Glycodendrimers and Influence of Architecture on Reactivity to a Lectin. *Proc. Natl. Acad. Sci. U. S. A.* **2016**, *113* (5), 1162−1167.
(26) Zhang, S.; Xiao, Q.; Sherman, S. E.; Muncan, A.; Ramos Vicente, A. D. M.; Wang, Z.; Hammer, D. A.; Williams, D.; Chen, Y.; Pochan, D. J.; Vertesy, S.; Andre, S.; Klein, M. L.; Gabius, H.-J.; Percec, V. Glycodendrimersomes from Sequence-Defined Janus Glycodendrimers Reveal High Activity and Sensor Capacity for the Agglutination by Natural Variants of Human Lectins. *J. Am. Chem. Soc.* **2015**, *137* (41), 13334−13344.
(27) Zhang, S.; Moussodia, R.-O.; Sun, H.-J.; Leowanawat, P.; Muncan, A.; Nusbaum, C. D.; Chelling, K. M.; Heiney, P. a.; Klein, M. L.; André, S.; Roy, R.; Gabius, H.-J.; Percec, V. Mimicking Biological Membranes with Programmable Glycan Ligands Self-Assembled from Amphiphilic Janus Glycodendrimers. *Angew. Chem., Int. Ed.* **2014**, *53* (41), 10899−10903.
(28) Percec, V.; Leowanawat, P.; Sun, H. J.; Kulikov, O.; Nusbaum, C. D.; Tran, T. M.; Bertin, A.; Wilson, D. A.; Peterca, M.; Zhang, S.; Kamat, N. P.; Vargo, K.; Moock, D.; Johnston, E. D.; Hammer, D. A.; Pochan, D. J.; Chen, Y.; Chabre, Y. M.; Shiao, T. C.; Bergeron-Brlek, M.; Andre, S.; Roy, R.; Gabius, H.-J.; Heiney, P. A. Modular Synthesis of Amphiphilic Janus Glycodendrimers and Their Self-Assembly into Glycodendrimersomes and Other Complex Architectures with Bioactivity to Biomedically Relevant Lectins. *J. Am. Chem. Soc.* **2013**, *135* (24), 9055−9077.
(29) Xiao, Q.; Rubien, J. D.; Wang, Z.; Reed, E. H.; Hammer, D. A.; Sahoo, D.; Heiney, P. A.; Yadavalli, S. S.; Goulian, M.; Wilner, S. E.; Baumgart, T.; Vinogradov, S. A.; Klein, M. L.; Percec, V. Self-Sorting and Coassembly of Fluorinated, Hydrogenated, and Hybrid Janus Dendrimers into Dendrimersomes. *J. Am. Chem. Soc.* **2016**, *138* (38), 12655−12663.
(30) Sherman, S. E.; Xiao, Q.; Percec, V. Mimicking Complex Biological Membranes and Their Programmable Glycan Ligands with Dendrimersomes and Glycodendrimersomes. *Chem. Rev.* **2017**, *117* (9), 6538−6631.
(31) Kopitz, J.; Xiao, Q.; Ludwig, A. K.; Romero, A.; Michalak, M.; Sherman, S. E.; Zhou, X.; Dazen, C.; Vértesy, S.; Kaltner, H.; Klein, M. L.; Gabius, H.-J.; Percec, V. Reaction of a Programmable Glycan Presentation of Glycodendrimersomes and Cells with Engineered Human Lectins To Show the Sugar Functionality of the Cell Surface. *Angew. Chem., Int. Ed.* **2017**, *56* (46), 14677−14681.
(32) Xiao, Q.; Yadavalli, S. S.; Zhang, S.; Sherman, S. E.; Fiorin, E.; da Silva, L.; Wilson, D. A.; Hammer, D. A.; André, S.; Gabius, H.-J.; Klein, M. L.; Goulian, M.; Percec, V. Bioactive Cell-like Hybrids Coassembled from (Glyco)Dendrimersomes with Bacterial Membranes. *Proc. Natl. Acad. Sci. U. S. A.* **2016**, *113* (9), E1134−E1141.
(33) Xiao, Q.; Ludwig, A.-K.; Romanò, C.; Buzzacchera, I.; Sherman, S. E.; Vetro, M.; Vértesy, S.; Kaltner, H.; Reed, E. H.; Möller, M.; Wilson, C. J.; Hammer, D. A.; Oscarson, S.; Klein, M. L.; Gabius, H.-J.; Percec, V. Exploring Functional Pairing between Surface Glycoconjugates and Human Galectins Using Programmable Glycodendrimersomes. *Proc. Natl. Acad. Sci. U. S. A.* **2018**, *115* (11), E2509−E2518.
(34) Rosen, B. M.; Wilson, C. J.; Wilson, D. A.; Peterca, M.; Imam, M. R.; Percec, V. Dendron-Mediated Self-Assembly, Disassembly, and Self-Organization of Complex Systems. *Chem. Rev.* **2009**, *109* (11), 6275−6540.
(35) Xiao, Q.; Wang, Z.; Williams, D.; Leowanawat, P.; Peterca, M.; Sherman, S. E.; Zhang, S.; Hammer, D. A.; Heiney, P. A.; King, S. R.; Markovitz, D. M.; Andre, S.; Gabius, H.-J.; Klein, M. L.; Percec, V. Why Do Membranes of Some Unhealthy Cells Adopt a Cubic Architecture? *ACS Cent. Sci.* **2016**, *2* (12), 943−953.
(36) Zhang, S.; Sun, H.-J.; Hughes, A. D.; Moussodia, R.-O.; Bertin, A.; Chen, Y.; Pochan, D. J.; Heiney, P. A.; Klein, M. L.; Percec, V. Self-Assembly of Amphiphilic Janus Dendrimers into Uniform Onion-like Dendrimersomes with Predictable Size and Number of Bilayers. *Proc. Natl. Acad. Sci. U. S. A.* **2014**, *111* (25), 9058−9063.
(37) Zhang, S.; Sun, H. J.; Hughes, A. D.; Draghici, B.; Lejnieks, J.; Leowanawat, P.; Bertin, A.; Otero De Leon, L.; Kulikov, O. V.; Chen, Y.; Pochan, D. J.; Heiney, P. A.; Percec, V. "Single-Single" Amphiphilic Janus Dendrimers Self-Assemble into Uniform Dendrimersomes with Predictable Size. *ACS Nano* **2014**, *8* (2), 1554−1565.
(38) Peterca, M.; Percec, V.; Leowanawat, P.; Bertin, A. Predicting the Size and Properties of Dendrimersomes from the Lamellar Structure of Their Amphiphilic Janus Dendrimers. *J. Am. Chem. Soc.* **2011**, *133* (50), 20507−20520.
(39) Röglin, L.; Lempens, E. H. M.; Meijer, E. W. A Synthetic "Tour de Force": Well-Defined Multivalent and Multimodal Dendritic Structures for Biomedical Applications. *Angew. Chem., Int. Ed.* **2011**, *50* (1), 102−112.
(40) Selin, M.; Peltonen, L.; Hirvonen, J.; Bimbo, L. M. Dendrimers and Their Supramolecular Nanostructures for Biomedical Applications. *J. Drug Delivery Sci. Technol.* **2016**, *34*, 10−20.
(41) Auvinen, H.; Zhang, H.; Nonappa; Kopilow, A.; Niemelä, E. H.; Nummelin, S.; Correia, A.; Santos, H. A.; Linko, V.; Kostiainen, M. A. Protein Coating of DNA Nanostructures for Enhanced Stability and Immunocompatibility. *Adv. Healthcare Mater.* **2017**, *6* (18), 1700692.
(42) Meyers, S. R.; Juhn, F. S.; Griset, A. P.; Luman, N. R.; Grinstaff, M. W. V. Anionic Amphiphilic Dendrimers as Antibacterial Agents. *J. Am. Chem. Soc.* **2008**, *130* (44), 14444−14445.
(43) Ghobril, C.; Charoen, K.; Rodriguez, E. K.; Nazarian, A.; Grinstaff, M. W. A Dendritic Thioester Hydrogel Based on Thiol-Thioester Exchange as a Dissolvable Sealant System for Wound Closure. *Angew. Chem., Int. Ed.* **2013**, *52* (52), 14070−14074.
(44) Nummelin, S.; Liljeström, V.; Saarikoski, E.; Ropponen, J.; Nykänen, A.; Linko, V.; Seppälä, J.; Hirvonen, J.; Ikkala, O.; Bimbo, L. M.; Kostiainen, M. A. Self-Assembly of Amphiphilic Janus Dendrimers into Mechanically Robust Supramolecular Hydrogels for Sustained Drug Release. *Chem. - Eur. J.* **2015**, *21* (41), 14433−14439.

DOI: 10.1021/acs.biomac.8b00931
Biomacromolecules 2018, 19, 3983−3993

(45) Arseneault, M.; Wafer, C.; Morin, J.-F. Recent Advances in Click Chemistry Applied to Dendrimer Synthesis. *Molecules* **2015**, *20* (5), 9263−9294.
(46) Wu, P.; Malkoch, M.; Hunt, J. N.; Vestberg, R.; Kaltgrad, E.; Finn, M. G.; Fokin, V. V.; Sharpless, K. B.; Hawker, C. J. Multivalent, Bifunctional Dendrimers Prepared by Click Chemistry. *Chem. Commun.* **2005**, No. 46, 5775−5777.
(47) Liu, P.; Viitala, T.; Kartal-Hodzic, A.; Liang, H.; Laaksonen, T.; Hirvonen, J.; Peltonen, L. Interaction Studies between Indomethacin Nanocrystals and PEO/PPO Copolymer Stabilizers. *Pharm. Res.* **2015**, *32* (2), 628−639.
(48) Van Eerdenbrugh, B.; Vermant, J.; Martens, J. A.; Froyen, L.; Van Humbeeck, J.; Augustijns, P.; Van Den Mooter, G. A Screening Study of Surface Stabilization during the Production of Drug Nanocrystals. *J. Pharm. Sci.* **2009**, *98* (6), 2091−2103.
(49) Liu, P.; Rong, X.; Laru, J.; Van Veen, B.; Kiesvaara, J.; Hirvonen, J.; Laaksonen, T.; Peltonen, L. Nanosuspensions of Poorly Soluble Drugs: Preparation and Development by Wet Milling. *Int. J. Pharm.* **2011**, *411* (1−2), 215−222.
(50) Surwase, S. A.; Boetker, J. P.; Saville, D.; Boyd, B. J.; Gordon, K. C.; Peltonen, L.; Strachan, C. J. Indomethacin: New Polymorphs of an Old Drug. *Mol. Pharmaceutics* **2013**, *10* (12), 4472−4480.
(51) Chokshi, R. J.; Sandhu, H. K.; Iyer, R. M.; Shah, N. H.; Malick, A. W.; Zia, H. Characterization of Physico-Mechanical Properties of Indomethacin and Polymers to Assess Their Suitability for Hot-Melt Extrusion Processs as a Means to Manufacture Solid Dispersion/Solution. *J. Pharm. Sci.* **2005**, *94* (11), 2463−2474.
(52) Bakatselou, V.; Oppenheim, R. C.; Dressman, J. B. Solubilization and Wetting Effects of Bile Salts on the Dissolution of Steroids. *Pharm. Res.* **1991**, *8* (12), 1461−1469.
(53) Fox, H. W.; Zisman, W. A. The Spreading of Liquids on Low-Energy Surfaces. III. Hydrocarbon Surfaces. *J. Colloid Sci.* **1952**, *7* (4), 428−442.
(54) Girifalco, L. A.; Good, R. J. A Theory for the Estimation of Surface and Interfacial Energies. I. Derivation and Application to Interfacial Tension. *J. Phys. Chem.* **1957**, *61* (7), 904−909.
(55) Sarnes, A.; Østergaard, J.; Jensen, S. S.; Aaltonen, J.; Rantanen, J.; Hirvonen, J.; Peltonen, L. Dissolution Study of Nanocrystal Powders of a Poorly Soluble Drug by UV Imaging and Channel Flow Methods. *Eur. J. Pharm. Sci.* **2013**, *50* (3−4), 511−519.
(56) Wassvik, C. M.; Holmén, A. G.; Bergström, C. A. S.; Zamora, I.; Artursson, P. Contribution of Solid-State Properties to the Aqueous Solubility of Drugs. *Eur. J. Pharm. Sci.* **2006**, *29* (3−4), 294−305.
(57) Inagi, T.; Muramatsu, T.; Nagai, H.; Terada, H. Mechanism of Indomethacin Partition between N-Octanol and Water. *Chem. Pharm. Bull.* **1981**, *29* (8), 2330−2337.
(58) Najib, N. M.; Suleiman, M. S. The Effect of Hydrophilic Polymers and Surface Active Agents on the Solubility of Indomethacin. *Int. J. Pharm.* **1985**, *24* (2−3), 165−171.
(59) Aceves-Hernandez, J. M.; Nicolás-Vázquez, I.; Aceves, F. J.; Hinojosa-Torres, J.; Paz, M.; Castañ O, V. M. Indomethacin Polymorphs: Experimental and Conformational Analysis. *J. Pharm. Sci.* **2009**, *98* (7), 2448−2463.
(60) Liu, P.; De Wulf, O.; Laru, J.; Heikkilä, T.; van Veen, B.; Kiesvaara, J.; Hirvonen, J.; Peltonen, L.; Laaksonen, T. Dissolution Studies of Poorly Soluble Drug Nanosuspensions in Non-Sink Conditions. *AAPS PharmSciTech* **2013**, *14* (2), 748−756.
(61) Bisrat, M.; Nyström, C. Physicochemical Aspects of Drug Release. VIII. The Relation between Particle Size and Surface Specific Dissolution Rate in Agitated Suspensions. *Int. J. Pharm.* **1988**, *47* (1−3), 223−231.
(62) Keck, C. M.; Müller, R. H. Drug Nanocrystals of Poorly Soluble Drugs Produced by High Pressure Homogenisation. *Eur. J. Pharm. Biopharm.* **2006**, *62* (1), 3−16.
(63) Simonelli, A. P.; Mehta, S. C.; Higuchi, W. I. Inhibition of Sulfathiazole Crystal Growth by Polyvinylpyrrolidone. *J. Pharm. Sci.* **1970**, *59* (5), 633−638.
(64) Ricarte, R. G.; Li, Z.; Johnson, L. M.; Ting, J. M.; Reineke, T. M.; Bates, F. S.; Hillmyer, M. A.; Lodge, T. P. Direct Observation of Nanostructures during Aqueous Dissolution of Polymer/Drug Particles. *Macromolecules* **2017**, *50* (8), 3143−3152.

DOI: 10.1021/acs.biomac.8b00931
Biomacromolecules 2018, 19, 3983−3993